



CHORUS

This is the accepted manuscript made available via CHORUS. The article has been published as:

Majorana flat bands and unidirectional Majorana edge states in gapless topological superconductors

Chris L. M. Wong, Jie Liu, K. T. Law, and Patrick A. Lee

Phys. Rev. B **88**, 060504 — Published 5 August 2013

DOI: [10.1103/PhysRevB.88.060504](https://doi.org/10.1103/PhysRevB.88.060504)

Majorana Flat Bands and Uni-directional Majorana Edge States in Gapless Topological Superconductors

Chris L. M. Wong¹, Jie Liu¹, K. T. Law¹ and Patrick A. Lee²

¹. Department of Physics, Hong Kong University of Science and Technology, Clear Water Bay, Hong Kong, China

². Department of Physics, Massachusetts Institute of Technology, Cambridge, MA, USA

In this work, we show that an in-plane magnetic field can drive a fully gapped $p \pm ip$ topological superconductor into a gapless phase which supports Majorana flat bands (MFBs). Unlike previous examples, the MFBs in the gapless regime are protected from disorder by a chiral symmetry. In addition, novel uni-directional Majorana edge states (MESs) which propagate in the same direction on opposite edges appear when the chiral symmetry is broken by Rashba terms. Unlike the usual chiral or helical edge states, uni-directional MESs appear only in systems with a gapless bulk. The MFBs and the uni-directional MESs induce nearly quantized zero bias conductance in tunneling experiments.

PACS numbers:

I. INTRODUCTION

A topological superconductor (TS) has a bulk superconducting gap and topologically protected gapless boundary states [1–5]. TSs are under intense theoretical and experimental studies due to the possibility of realizing Majorana fermions in these systems, which act as their own antiparticles and obey non-Abelian statistics [6–8]. Majorana fermions in TSs are topologically protected, in the sense that the Majorana fermions cannot be removed by perturbations unless the bulk energy gap is closed or certain symmetries are broken.

Remarkably, recent development shows that Majorana fermions exist in systems where the bulk is gapless [9–20]. For example, Majorana edge states (MESs) with flat dispersion can be found in 2D nodal $d_{xy} + p$ -wave superconductors which respect time-reversal symmetry [10–12]. It is also shown that zero energy Majorana flat bands (MFBs) can appear on the surface of 3D time-reversal invariant non-centrosymmetric superconductors which have topologically stable line nodes in the bulk [13–15].

In this work, we show that an in-plane magnetic field can drive a fully gapped $p \pm ip$ -wave TS into a gapless regime which supports symmetry protected MFBs. An in-plane magnetic field may first close the bulk gap. Further increasing the strength of the magnetic field creates zero energy MFBs in the excitation spectrum when the bulk is gapless. The evolution of the excitation spectrum of a $p \pm ip$ -wave superconductor as a function of the in-plane magnetic field strength is shown in Fig.1. and Fig.2. Unlike the MFBs discussed in previous works [10–15] which are not protected against disorder, *the MFBs discussed in this work are protected by a chiral symmetry and the zero energy modes stay at zero energy even in the presence of disorder.*

S-wave pairing and Rashba spin-orbit coupling terms break the chiral symmetry which protects the MFBs. In this case, uni-directional MESs, which are distinct from the usual helical or chiral MESs in that the modes on

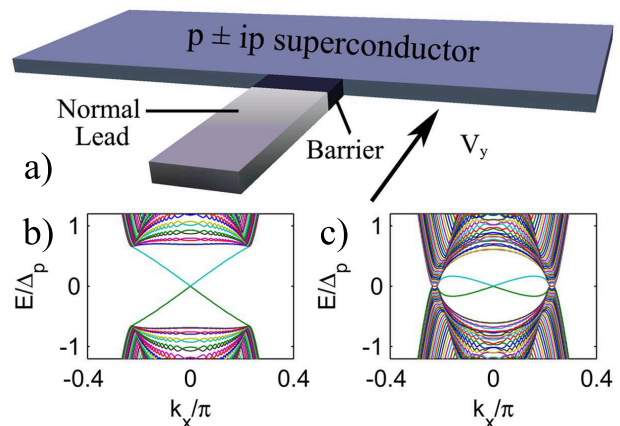


FIG. 1: a) A schematic picture of a $p \pm ip$ -wave superconductor subject to an in-plane magnetic field V_y . A tunnel junction and a normal lead N is attached to the superconductor. b) The energy spectrum of a $p \pm ip$ superconductor in the topologically non-trivial regime. Periodic boundary conditions in the x -direction and open boundary conditions in the y -direction are assumed. The parameters are $t = 12\Delta_p$, $\mu = 3\Delta_p - 2t$, $\Delta_s = 0$, $\alpha_R = 0$ and $V_y = 0$. c) Same parameters as b), except $V_y = 0.7\Delta_p$. The bulk energy gap is closed in this regime.

opposite edges move in the same direction, may appear. Interestingly, this new type of edge states can only appear in systems with a gapless bulk which are different from chiral or helical edge states which appear in systems with a bulk gap. Finally, we show that the MESs induce nearly quantized zero bias conductance in tunneling experiments.

II. MAJORANA FLAT BANDS

We start with a BdG Hamiltonian which describes a two-dimensional non-centrosymmetric superconductor with both spin-triplet $p_x + ip_y$ -wave, spin-singlet s -wave

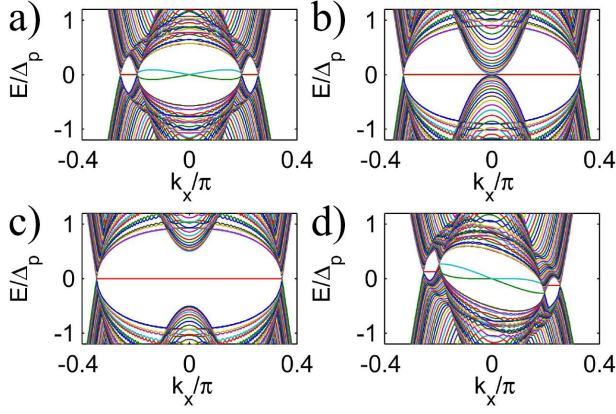


FIG. 2: The evolution of the energy spectrum of a $p \pm ip$ -wave superconductor as V_y increases. For a) to c) the parameters are the same as Fig.1b except the values of V_y . a) $V_y = \Delta_p$. b) $V_y = 3\Delta_p$. c) $V_y = 3.5\Delta_p$. d) S-wave pairing and Rashba terms with $\Delta_s = 0.3\Delta_p$ and $\alpha_R = 0.2\Delta_p$ are added to a).

pairing and Rashba spin-orbit coupling in the presence of a magnetic field.

$$H_p(\mathbf{k}) = \begin{pmatrix} \xi(\mathbf{k}) + \mathbf{V} \cdot \boldsymbol{\sigma} & \hat{\Delta}(\mathbf{k}) \\ \hat{\Delta}^\dagger(\mathbf{k}) & -\xi^T(-\mathbf{k}) - \mathbf{V} \cdot \boldsymbol{\sigma}^* \end{pmatrix}. \quad (1)$$

Here $\xi(\mathbf{k}) = [-t(\cos k_x + \cos k_y) - \mu]\sigma_0 - \alpha_R[-\sin k_y\sigma_x + \sin k_x\sigma_y]$ is the sum of the kinetic energy and the Rashba spin-orbit coupling, \mathbf{V} describes the Zeeman coupling of the electrons with an external magnetic field, $\hat{\Delta}(\mathbf{k}) = (\Delta_s + \mathbf{d}(\mathbf{k}) \cdot \boldsymbol{\sigma})(i\sigma_y)$ is the superconducting gap function. We first assume that the spin-singlet pairing amplitude Δ_s and the Rashba spin-orbit coupling α_R are zero. The spin-triplet pairing vector is chosen as $\mathbf{d}(\mathbf{k}) = \Delta_p(-\sin k_y, \sin k_x, 0)$ such that the Hamiltonian describes a two dimensional, helical, $p \pm ip$ -wave superconductor where Δ_p is a constant. When $\mathbf{V} = 0$, the Hamiltonian respects both time-reversal symmetry $T = U_T K$ with $U_T^{-1} H_p^*(\mathbf{k}) U_T = H_p(-\mathbf{k})$ and particle-hole symmetry $P = U_P K$ with $U_P^{-1} H_p^*(\mathbf{k}) U_P = -H_p(-\mathbf{k})$. Here, K is the complex conjugate operator, $U_T = \sigma_0 \otimes i\sigma_y$ and $U_P = \sigma_x \otimes \sigma_0$ such that $T^2 = -1$ and $P^2 = 1$.

According to symmetry classification, the above Hamiltonian in the absence of an external magnetic field belongs to DIII class which can be topologically non-trivial. In the topologically non-trivial regime where $|\mu| < |4t|$ and $|\Delta_p| > |\Delta_s|$, the superconductor possesses gapless counter-propagating helical MESs. The energy spectrum in the topologically non-trivial regime is shown in Fig.1b. In the rest of this section, we show that the $p \pm ip$ superconductor responds to an in-plane magnetic field in an anomalous way as described in the *Introduction*.

To be specific, we suppose a magnetic field is applied in the y -direction such that $\mathbf{V} = (0, V_y, 0)$. In the presence of a magnetic field, the time-reversal symmetry $T = U_T K$ is broken. However, the Hamiltonian satisfies

a time-reversal like symmetry $T_{1d} = U_{T_{1d}} K$ such that $T_{1d}^{-1} H(k_x, k_y) T_{1d} = H(k_x, -k_y)$, where $U_{T_{1d}} = \sigma_z \otimes \sigma_z$. Moreover, the Hamiltonian satisfies a particle-hole like symmetry $P_{1d} = U_{P_{1d}} K$ such that $P_{1d}^{-1} H(k_x, k_y) P_{1d} = -H(k_x, -k_y)$ with $U_{P_{1d}} = \sigma_y \otimes \sigma_y$. Since the symmetry operators operate on k_y only and k_x is unchanged, one may regard k_x as a tuning parameter and the Hamiltonian can be written as $H_{k_x}(k_y)$. As $H_{k_x}(k_y)$ respects the symmetries T_{1d} and P_{1d} with $T_{1d}^2 = P_{1d}^2 = 1$, $H_{k_x}(k_y)$ is a BDI class Hamiltonian which can be classified by an integer.

To classify the Hamiltonian $H_{k_x}(k_y)$ with k_x as a tuning parameter, we note that as a result of the T_{1d} and P_{1d} symmetries, $H_{k_x}(k_y)$ satisfies the chiral symmetry $S_{1d} = T_{1d} P_{1d}$ with

$$S_{1d}^{-1} H(k_x, k_y) S_{1d} = -H(k_x, k_y). \quad (2)$$

In this case, $H_{k_x}(k_y)$ can be off-diagonalized in the basis which diagonalizes S_{1d} such that

$$\tilde{H}_{k_x}(k_y) = \begin{pmatrix} 0 & A_{k_x}(k_y) \\ A_{k_x}^\dagger(k_y) & 0 \end{pmatrix}. \quad (3)$$

Defining the quantity

$$z(k) = e^{i\theta(k)} = \text{Det}[A_{k_x}(k)] / |\text{Det}[A_{k_x}(k)]|, \quad (4)$$

the winding number of $\theta(k)$, can be used as the topological invariant which characterizes the Hamiltonian $H_{k_x}(k_y)$. The winding number N_{BDI} can be written as^{12,21}

$$N_{BDI} = \frac{-i}{\pi} \int_{k_y=0}^{k_y=\pi} \frac{dz(k_y)}{z(k_y)}. \quad (5)$$

Using $A_{k_x}(k_y)$ obtained from $H_{k_x}(k_y)$, we have $|N_{BDI}| = 1$ when

$$\begin{aligned} \mathcal{M}(k_x, k_y=0) \mathcal{M}(k_x, k_y=\pi) &< 0, \quad \text{where} \\ \mathcal{M}(k_x, k_y) &= [\mu + t(\cos k_x + \cos k_y)]^2 + \Delta_p^2 \sin^2 k_x - V_y^2, \end{aligned} \quad (6)$$

assuming that V_y and Δ_p are non-zero. In the range of k_x where $N_{BDI} = 1$, the Hamiltonian $H_{k_x}(k_y)$ is topologically nontrivial. For a $p \pm ip$ superconductor with periodic boundary conditions in the x -direction and open boundary conditions in the y -direction, there are zero energy Majorana modes localized on the edges of the system when Eq.6 is satisfied. Therefore, MFBs appear in the corresponding parameter regime.

The evolution of the energy spectrum of a $p \pm ip$ superconductor as a result of an increasing in-plane magnetic field is shown in Fig.1 and Fig.2. First, an in-plane magnetic field reduces the bulk gap as shown in Fig.1c. Second, after the bulk gap is closed, MFBs appear for a finite range of k_x where $|N_{BDI}| = 1$ (Fig.2a). Third, by further increasing the magnetic field, the bulk gap at $k_x = 0$ is closed (Fig.2b). Fourth, by increasing the magnetic field even further, the energy crossing at $k_x = 0$

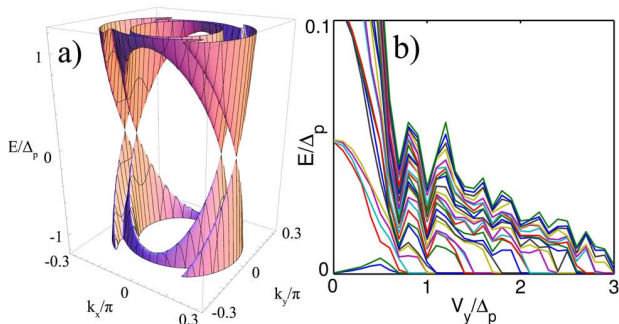


FIG. 3: a) The bulk energy spectrum of a $p \pm ip$ superconductor. The parameters are the same as the ones in Fig.2a but periodic boundary conditions in both the x and y directions are imposed. b) The energy spectrum of a pure $p \pm ip$ -wave superconductor with dimensions $L_x = 100a$ and $L_y = 300a$, where a is the lattice spacing. Only the thirty lowest energy eigenvalues are shown. Periodic boundary conditions in the x -direction and open boundary conditions in the y -direction are assumed. On-site Gaussian disorder with variance $w^2 = (1.5\Delta_p)^2$ is present. It is evident that as V_y increases, states collapse to zero energy and stay there, increasing the number of zero energy modes. This indicates the widening of the MFBs as V_y increases. Importantly, the zero energy Majorana modes are not lifted by disorder.

disappears and only a MFB remains (Fig.2c). It is important to note that the MFBs appear when the bulk is gapless. The bulk energy spectrum of a $p \pm ip$ -wave superconductor corresponding to Fig.2a is shown in Fig.3a. It is evident that there are nodal points in the bulk spectrum when MFBs appear. The nodal points in Fig.2a are the projection of the bulk nodal points on the k_x -axis in Fig.3a, similar to the cases in intrinsic gapless TSs [12,15,19]. Both the nodal points in the bulk spectrum as well as the MFBs are protected by the topological invariant N_{BDI} . In other words, the MFBs and the nodal points in the bulk appear whenever N_{BDI} is non-trivial for some range of k_x . The results in this section applies to helical superconductors/superfluids with d -vector $\mathbf{d}(\mathbf{k}) = (\sin k_x, \sin k_y, 0)$ as well. One example of such a helical superfluid is Helium 3 B-phase.

III. UNI-DIRECTIONAL MAJORANA EDGE STATES

It is shown above that MFBs appear when $N_{BDI} = 1$ for a finite range of k_x and the MFBs are protected by the symmetries P_{1d} and T_{1d} . However, s-wave pairing and Rashba terms break the chiral symmetry S_{1d} in Eq.2 and lift the zero energy modes to finite energy as shown in Fig.2d. In the case of adding s-wave and Rashba terms to Fig.2c, the MFB acquires a finite slope and uni-directional MESs appear at the sample edge as shown in Fig.4a. A schematic picture of the uni-directional MESs is shown in the insert.

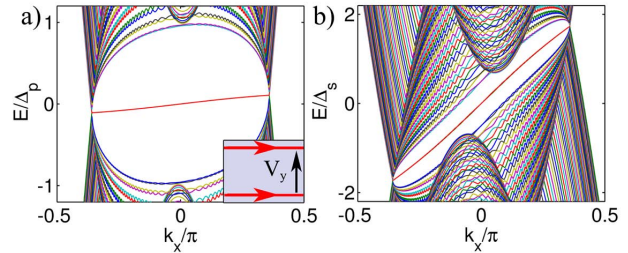


FIG. 4: a) The parameters are the same as those in Fig.2d except the values of V_y . The MFB acquires a finite slope when Δ_s and α_R are finite at $V_y = 4\Delta_p$. Uni-directional MESs appear in this regime. A schematic picture of the uni-directional MESs is shown in the insert. b) The energy spectrum of the case with $\Delta_p = 0$, $t = 12\Delta_s$, $\mu = 3\Delta_s - 2t$ and $\alpha_R = 2\Delta_s$.

We point out that the right moving edge modes are compensated by extra left moving modes in the bulk, so the current on the edge is cancelled by a backflow current in the bulk. Since a bulk backflow current is required to compensate for the edge current, the uni-directional edge states can only appear in systems with a gapless bulk. This is different from chiral and helical edge states which appear in systems with a bulk gap. In the presence of the s-wave pairing and Rashba spin-orbit coupling, the Hamiltonian in Eq.1 describes non-centrosymmetric superconductors such as CePt₃Si, CeIrSi₃ and CeRhSi₃ and these materials are candidates for realizing the uni-directional edge states.

Another interesting finding is that the uni-directional MESs can appear in the absence of $p \pm ip$ -wave pairing. The energy spectrum of an s-wave superconductor with Rashba terms and finite V_y is shown in Fig.4b. It can be shown that the uni-directional edge states appear when

$$\mathcal{M}_s(0,0)\mathcal{M}_s(0,\pi) < 0, \quad \text{where} \\ \mathcal{M}_s(k_x, k_y) = [\mu + t(\cos k_x + \cos k_y)]^2 + \Delta_s^2 - V_y^2. \quad (7)$$

The systems with pure s-wave pairing and Rashba terms can be realized by inducing s-wave superconductivity in semi-conductors as demonstrated in recent experiments [22–24].

IV. ANDREEV REFLECTION AND EFFECTS OF DISORDER

It has been shown in previous works that Majorana fermions induce resonant Andreev reflection at the junction between a normal lead and a fully gapped TS [25,26]. However, resonant Andreev reflection may not happen when the bulk is gapless due to the non-vanishing direct tunneling amplitudes from the normal lead to the gapless superconductor. In this section, we calculate the zero bias conductance (ZBC) of a junction between a normal lead and a TS as a function of the in-plane magnetic field strength. It is found that MFBs and uni-directional

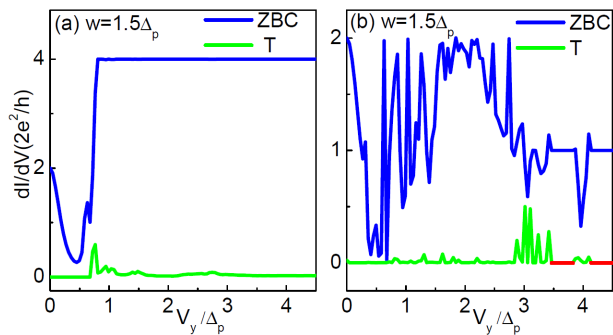


FIG. 5: The ZBC versus V_y . a) ZBC from a lead to a $p \pm ip$ -wave superconductor. The setup is depicted in Fig.1a. The superconductor has dimensions $L_x = 100a$ and $L_y = 300a$. Periodic boundary conditions in the x-direction is assumed. $t = 12\Delta_p$, $\mu = 3\Delta_p - 2t$ in the superconductor and the lead. The barrier between the lead and the superconductor is simulated by a reduced hopping amplitude $t_c = 0.3t$. A semi-infinite lead with width $8a$ is used in the simulation. The number of conducting channels in the lead is $N_c = 4$. The direct tunneling contribution to the ZBC is denoted as T . Gaussian on-site disorder with variance $w^2 = (1.5\Delta_p)^2$ is present. b) S-wave pairing and Rashba terms with $\Delta_s = 0.3\Delta_p$ and $\alpha_R = 0.2\Delta_p$ are added to a). The red lines near $V_y = 4\Delta_p$ indicate the regime where the ZBC is quantized due to the presence of the uni-directional MESs.

MESs induce nearly quantized ZBC even when the bulk is gapless and in the presence of disorder.

A schematic picture of the experimental setup is shown in Fig.1a. A normal lead is coupled to an edge of the TS to form a tunnel junction. Using the lattice Green's function method [27–29], we calculate the direct tunneling amplitude and the Andreev reflection amplitude of the tunnel junction.

Fig.5a shows the ZBC as a function of V_y for a $p \pm ip$ -wave superconductor in the presence of on-site disorder. To understand the results, we note that time-reversal symmetry is preserved and the system is fully gapped at $V_y = 0$, the $4e^2/h$ quantization of ZBC is the property of a DIII class TS which has two Majorana zero modes on the edge [30,31]. As V_y increases, time-reversal symmetry is broken and the ZBC is suppressed by disorder. Further increasing V_y closes the bulk gap and there is a large jump in the ZBC. This jump is due to the contribution from the Andreev reflection caused by the MFBs and the direct tunneling caused by the gapless bulk. This can be clearly seen from the V_y dependence of T in Fig.5a. It is interesting to note that the final ZBC is almost quantized at $\frac{2e^2}{h}N_c$ with $N_c = 4$, where N_c is the number of conducting channels in the normal lead. This is due to the Andreev reflection caused by the large number of independent Majorana fermions from the flat band.

The nearly quantized ZBC in the presence of disorder at large V_y in Fig.5a suggests that the MFBs are robust against disorder. To confirm this, the energy spectrum of the $p \pm ip$ superconductor with parameters corresponding to Fig.5a is shown in Fig.3b. It is evident from Fig.3b

that finite energy states collapse to zero energy and stay there, increasing the number of zero energy modes as V_y increases. A detailed account of the robustness of the MFBs is given in next section.

Fig.5b shows the ZBC versus V_y when s-wave pairing and Rashba terms are added to Fig.5a. There are ZBC plateaus near $V_y = 4\Delta_p$ in this case. However, the ZBC is quantized at $\frac{2e^2}{h}$ due to the presence of only one zero energy edge mode on the edge when a MFB becomes an uni-directional edge state in this regime.

V. ROBUSTNESS OF MAJORANA FLAT BANDS

It is evident from Fig.3b that the MFBs are robust against disorder. In this section, we argue that the MFBs are protected by the chiral symmetry S_{1d} in Eq.2.

In our case, the zero energy edge states localized on the same edge of the sample have the same chirality. The chirality of an eigenstate of S_{1d} is defined as the eigenvalue of the state with respect to S_{1d} which is always $+1$ or -1 . Therefore, the net chirality number of an edge, which is the sum of the chirality numbers of all the zero energy states localized on the edge, is always non-zero when MFBs appear.

Moreover, it can be shown that the number of stable zero energy modes on an edge equals to the net chirality number of the edge [12]. Since on-site disorder does not break the chiral symmetry and cannot change the net chirality number, the number of stable zero energy modes cannot be changed by disorder. In contrast, in previous examples of MFB's [10,12] the net chirality number on each edge is zero.

To illustrate that the net chirality number on an edge is non-zero, we solve the eigenstates of the Hamiltonian in Eq.2. In the presence of an edge parallel to the x-direction at $y = 0$ and assuming that the superconductor is in the positive y -plane, $A_{k_x}(k_y)$ can be written as

$$\begin{pmatrix} iV_y - i\Delta \frac{\partial}{\partial y} + \Delta \frac{\partial}{\partial x} & -t(2 + \frac{1}{2} \frac{\partial^2}{\partial y^2} + \frac{1}{2} \frac{\partial^2}{\partial x^2}) - \mu \\ t(2 + \frac{1}{2} \frac{\partial^2}{\partial y^2} + \frac{1}{2} \frac{\partial^2}{\partial x^2}) + \mu & iV_y - i\Delta \frac{\partial}{\partial y} - \Delta \frac{\partial}{\partial x} \end{pmatrix}. \quad (8)$$

Using the ansatz $[0, 0, \alpha_-, \beta_-]^T \sin(a_- y) e^{-y/b_- + ik_x x}$ and $[\alpha_+, \beta_+, 0, 0]^T \sin(a_+ y) e^{-y/b_+ + ik_x x}$, we find two zero energy eigenstates for the Hamiltonian at $k_x = 0$ with $a_{\mp} = [2t(2t + \mu) - \Delta_p^2 \mp 2V_y t]/t^2$ and $b_{\mp} = \frac{t}{\Delta_p}$. As expected, the decay length b_{\mp} equals the superconducting coherence length. These two eigenstates are manifested as zero energy modes at $k_x = 0$ in Fig.2a and 2b.

Interestingly, when $V_y > |2t + \mu|$, a_- becomes imaginary and the corresponding wavefunction is not normalizable. As a result, only one zero energy mode with chirality $+1$ is left at $k_x = 0$ as shown in Fig.2c. It can be shown similarly that for large V_y , all the zero energy modes localized on one edge have the same chirality. As a result, the net chirality number on an edge is not zero

and the zero energy modes cannot be lifted by local perturbations which preserve the chirality number. Since V_x does not break the chiral symmetry, the MFBs can appear in the presence of V_x . However, V_z breaks the chiral symmetry that an out-of-plane magnetic field can destroy the MFBs.

VI. CONCLUSION

We show that an in-plane magnetic field can drive a $p \pm ip$ -wave superconductor to a gapless phase which supports chiral symmetry protected MFBs. In the presence of s-wave pairing and Rashba terms, novel uni-directional

MESs appear.

VII. ACKNOWLEDGMENTS

The authors thank A. Akhmerov, C. Beenakker, C. Kane, T.K. Ng, Y. Tanaka and especially M. Sato for inspiring discussions. CLMW, JL and KTL are supported by HKRGC through Grant 605512 and HKUST3/CRF09. PAL acknowledges the support from DOE Grant No. DEFG0203ER46076. He also thanks the Institute for Advanced Studies at HKUST for its hospitality.

-
- ¹ A. P. Schnyder, S. Ryu, A. Furusaki, A. W. W. Ludwig, Phys. Rev. B **78**, 195125 (2008).
² A. Kitaev, arXiv:0901.2686.
³ Jeffrey C.Y. Teo and C.L. Kane, Phys. Rev. B **82**, 115120 (2010).
⁴ X.L. Qi and S.C. Zhang, Rev. Mod. Phys. **83**, 1057-1110 (2011).
⁵ C.W.J. Beenakker, Annu. Rev. Con. Mat. Phys. **4**, 113 (2013).
⁶ N. Read and D. Green, Phys. Rev. B **61**, 10267 (2000).
⁷ A. Y. Kitaev, Physics-Uspekhi **44**, 131 (2001).
⁸ D. A. Ivanov, Phys. Rev. Lett. **86**, 268 (2001).
⁹ B. Beri, Phys. Rev. B **81**, 134515 (2010).
¹⁰ Y. Tanaka, Y. Mizuno, T. Yokoyama, K. Yada, M. Sato Phys. Rev. Lett. **105**, 097002 (2010).
¹¹ K. Yada, M. Sato, Y. Tanaka, T. Yokoyama, Phys. Rev. B **83**, 064505 (2011).
¹² M. Sato, Y. Tanaka, K. Yada, T. Yokoyama, Phys. Rev. B **83**, 224511 (2011).
¹³ A.P. Schnyder and S. Ryu, Phys. Rev. B **84**, 060504 (R) (2011).
¹⁴ P. M. R. Brydon, A. P. Schnyder and C. Timm, Phys. Rev. B **84**, 020501(R) (2011).
¹⁵ A. P. Schnyder, P. M. R. Brydon and Carsten Timm, Phys. Rev. B **85**, 024522 (2012).
¹⁶ M. Sato and S. Fujimoto, Phys. Rev. Lett. **105**, 217001 (2010).
¹⁷ Jay D. Sau, Sumanta Tewari, Physical Review B **86**, 104509 (2012).
¹⁸ T. Meng, L. Balents, Phys. Rev. B **86**, 054504 (2012).
¹⁹ F. Wang, D.H. Lee, Phys. Rev. B **86**, 094512 (2012).
²⁰ Y. Li and C. Wu, Sci. Rep. **2**, 392 (2012).
²¹ Sumanta Tewari, Jay D. Sau, Phys. Rev. Lett. **109**, 150408 (2012).
²² V. Mourik, K. Zuo, S.M. Frolov, S.R. Plissard, E.P.A.M. Bakkers, and L.P. Kouwenhoven, Science **336**, 1003 (2012).
²³ M. T. Deng, C.L. Yu, G.Y. Huang, M. Larsson, P. Caro, H.Q. Xu, arXiv:1204.4130 (2012).
²⁴ A. Das, Y. Ronen, Y. Most, Y. Oreg, M. Heiblum, H.Shtrikman, arXiv:1205.7073 (2012).
²⁵ K. T. Law, P. A. Lee, and T. K. Ng, Phys. Rev. Lett. **103**, 237001 (2009).
²⁶ M. Wimmer, A.R. Akhmerov, J.P. Dahlhaus, C.W.J. Beenakker, New J. Phys. **13**, 053016 (2011).
²⁷ P.A. Lee and D.S. Fisher, Phys. Rev. Lett. **47**, 882 (1981).
²⁸ D.S. Fisher and P.A. Lee Phys. Rev. B **23**, 6851 (1981).
²⁹ Q.F. Sun and X. C. Xie, J. Phys.: Condens. Matter **21** (2009) 344204.
³⁰ I. C. Fulga, F. Hassler, A. R. Akhmerov and C. W. J. Beenakker, Phys.Rev.B **83**, 155429 (2011).
³¹ C. L. M. Wong and K. T. Law, Phys. Rev. B **86**, 184516 (2012).